Enhanced Protection Scheme for Smart Grids Using Power Line Communications Techniques—Part I: Detection of High Impedance Fault Occurrence

Apostolos N. Milioudis, *Student Member, IEEE*, Georgios T. Andreou, *Member, IEEE*, and Dimitrios P. Labridis, *Senior Member, IEEE*

***Abstract*—Occurrence of high impedance faults (HIFs) in rural overhead power distribution networks may cause safety and economic issues for both public and the utility. Such faults may not be detected by the conventional protection schemes, so the development of a more sophisticated method is necessary. The forthcoming evolution of power networks to smart grids creates opportunities for new technologies to be implemented to that purpose. Utilities may transmit data that are necessary for the system operation using specific frequency ranges. A novel method utilizing these is proposed in this work. The monitoring of the network's input impedance in these frequency ranges can be used for detection of HIF occurrence, because such faults impose significant changes in its value. The proposed method is applied to single branch topologies, as well as to an existing topology of a Greek rural distribution system. Significant conclusions are derived in both cases. Moreover, the influence of several parameters, such as fault impedance and location and earth's electromagnetic properties on the method's efficacy is examined. Also, it is shown that the implementation of the proposed method may be drastically simplified by focusing on the monitoring of specific frequencies rather than the entire frequency range under study.**

***Index Terms*—High impedance fault detection, power distribution faults, power line communications, power system protection, smart grids.**

I. Introduction

POWER SYSTEM protection is an issue of high importance both for safety and functionality reasons. A perfect power system protection scheme should be able to ensure that no hazardous overvoltages will endanger human life or equipment operation under all circumstances. Naturally, the design and development of such a system would be either prohibitively expensive or even infeasible.

Power distribution networks are subject to various types of faults. The traditional protection concept is based on monitoring of the feeder currents and tripping of circuit breakers when a current exceeds a predetermined value, following a time response that depends on the measured current value. An operational point commonly used for the relay of a feeder's circuit breaker is close to twice the value of the maximum feeder load. However, the rise of the network current due to a fault depends mainly on the fault impedance value. Consequently, it is possible for a fault to exhibit a high impedance value, and merely cause a slight increase to the monitored feeder current. In such a case, the feeder protective equipment will fail to recognize the fault, as it will attribute the current rise to a change in the network load [1], leaving thus safety issues such as increased step voltages and the possibility of fire initiation unattended [2].

The necessity rises therefore for the development of an effective method, which will provide protection for a wide variety of faults, avoiding at the same time events that could lead to unnecessary circuit breaker tripping and the subsequent disconnection of feeders, as such situations would result in both financial and credibility loss for a power company. Such a protection scheme should ideally cover both fault detection and location.

To achieve this goal, utilities worldwide have been financing several projects over the last years. Within the context of research on protection schemes which could provide maximum functionality at minimum cost, the field of detecting low current faults has attracted intense research interest [3], [4]. Aucoin *et al.* have suggested models for the monitoring of high current components close to the main frequency value [5], [6], whereas Lee *et al.* have developed and installed a microprocessor data acquisition system [7], showing that constant impedance loads provide a sufficient load model for high impedance fault (HIF) calculations [8]. Furthermore, Balser *et al.* have proposed a model that utilizes the 1th, 3th, and 5th harmonics of the phase current, identifying the presence of HIF with the help of normalized symmetrical current components of each harmonic current [9]. In addition, the utilization of Bayesian selectivity [10], discrete wavelet transform [11]–[15], and artificial intelligence [16]–[19] for HIF detection may be found in the literature. However, all the aforementioned methods may offer fault detection, but they are incapable of determining the exact fault location.

Novel ways to overcome this problem may be offered by the forthcoming and very promising transformation of traditional electrical networks to smart grids, which is expected to revolutionize their operation [20]–[23]. Within this context, novel technologies are introduced aiming to improve the overall

Manuscript received July 14, 2011; revised October 12, 2011, February 13, 2012, May 09, 2012; accepted July 04, 2012. Date of publication October 23, 2012; date of current version December 28, 2012. This work was supported in part by the Greek State Scholarships Foundation (SSF). Paper no. TSG-00245-2011.

The authors are with the Department of Electrical and Computer Engineering, Aristotle University of Thessaloniki, 54124 Thessaloniki, Greece (e-mail: amilioud@auth.gr; gandreou@auth.gr; labridis@auth.gr).

Color versions of one or more of the figures in this paper are available online at http://ieeexplore.ieee.org.

Digital Object Identifier 10.1109/TSG.2012.2208987

system functionality by using equipment in order to combine the implementation of as many tasks as possible. Naturally, one of the most important tasks studied is the system protection [24], [25]. One of the technologies that may be used in order to improve the operation of power distribution networks is power line communications (PLC) [26]. More specifically, studies have shown that PLC systems may provide high speed data transmission [27]–[29], which may be utilized for the general communication purposes of a network. However, the same PLC devices could also be used for HIF detection, through their ability to superimpose high frequency signals on power networks.

Signal superposition was originally used in electrical networks for the transmission of important operational information. In this context, signals at frequencies that differed from the network main value (50, 60 Hz) were initially utilized on high voltage (HV) networks. This technique was implemented later on at the medium voltage (MV) and low voltage (LV) networks [30]. For protection purposes, signal superposition for the detection of low current faults has been suggested by Zamora *et al.* [31], utilizing considerably low frequencies, i.e., hundreds of Hertz [32]. The usage of these frequency range limits the efficacy of the method cause to harmonics produced by power electronics. Moreover, the methodology proposed in these works can only provide fault detection, and not location, as opposed to the work presented here. Moreover, in a previous work by the authors it was shown that the existence of a HIF on a transmission line may cause significant alteration to the line's input impedance at frequencies that lie into the Cenelec A Band (i.e., 9–95 kHz) frequency range, proposing thus a novel approach to HIF detection by signal superposition [33].

In this work, a novel method utilizing PLC techniques for the combined detection and location of HIF is proposed. More specifically, in Part I of the work, the concept of HIF detection with the utilization of the Cenelec A frequency band is thoroughly analyzed, whereas in Part II the respective concept of HIF location is presented. Considering Part I of the work, the effect of a HIF on a network's input impedance is thoroughly examined, taking into consideration all parameters which may interfere with the results. At first, the implementation scope of the proposed solution is presented, along with the network characteristics utilized. Consequently, the theoretical basis for the application of the method is presented. Within this context, the basic concepts of transmission line theory, on which the method effectiveness depends, are explained. Furthermore, the influence of the earth's electromagnetic properties on the method results is investigated. To this purpose, the method is applied firstly on simplified topologies with no branches, so as to apprehend the mechanisms, with which several parameters, such as the fault impedance and location, as well as the earth's resistivity and permittivity, affect its efficacy. Subsequently, the proposed method is applied on a real topology that is part of the Greek rural MV distribution network. In all cases, significant deviations between input impedances under normal and fault conditions are noticed, and important conclusions concerning the application of the method are derived.

II. Theoretical Analysis

A. Application Scope

The application scope of the proposed methodology includes the MV overhead power lines comprising parts of power distribution networks. A great portion of such a network consists of MV overhead power lines that cover large areas to deliver the energy needed by the consumers. These lines pass mainly through rural areas, and the occurrence of high impedance faults with the known dangerous outcomes is possible. MV overhead power lines are formed by three phase wires above a lossy ground plane. A HIF can exist between a phase wire and the ground. Thus, a signal injection between the phase wire and the ground plane may be used for the detection of such kind of faults, specifically by monitoring the input impedance of the circuit formed. Taking into account only those parts of the arrangement participating in the circuit formulation, the analysis is simplified to a single phase one.

The 20/0.4 kV transformers of the network separate it into distinct parts. Typically, the primary windings of the medium to low voltage transformers installed in the Greek distribution system are connected in delta, whereas the respective secondary windings are connected in star with a grounded neutral. The delta connection serves for the elimination of the third harmonic at the MV side and forces voltage balancing at the same time. On the other hand, the star connection with a grounded neutral at the LV side is for protection reasons and for connection of single phase consumers. In any case, for every known winding connection a grounded neutral at the MV side is unlikely, because it creates problems rather than offers functionality. Considering that the signal injection at the MV level for HIF detection is from phase to ground, these transformers behave as an open circuit at the frequencies used. This fact offers a complete isolation of the monitored area from the LV parts of the network, constraining it to the MV level only. Furthermore, the usage of frequencies within the frequency range of kHz provides complete independence from the operation of the network at the main frequency.

A typical Greek rural MV feeder consists of ACSR conductors of 70/12 mm^2 nominal cross section at a height of 10 m above the ground plane with distance of 1 m from each other. For the application of the proposed method, the calculation of the per unit length transmission line electric characteristics is necessary so as to determine the input impedance for various frequencies.

B. HIF Detection by Monitoring the Input Impedance

The initial attempt to approach the problem of detecting HIFs by using PLC techniques adopted the single conductor formulation instead of the multiconductor one. The presence of other conductors in the multiconductor case creates coupling between voltages and currents of all phases through electromagnetic interaction. Omitting this particular coupling in the single conductor case leads to a more clear observation and comprehension of the occurring traveling wave phenomena. This adaptation can provide the basis for the creation of a robust fault detection technique, and the complete understanding of the trans-

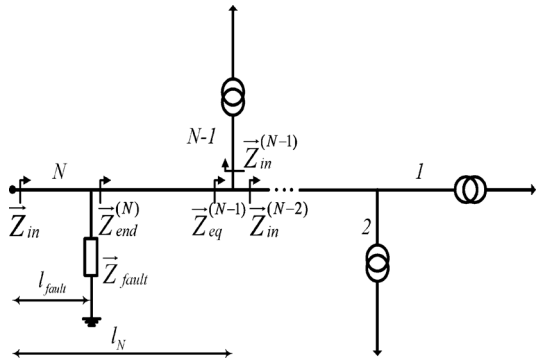

Fig. 1. Radial MV network topology with several branches.

mission line phenomena manifesting under HIF presence, and can be subsequently extended to the multiconductor case.

The input impedance of a single phase transmission line circuit that is terminated with an impedance $\overrightarrow{Z_l}$ is given by (1) [34]:

$$\overrightarrow{Z}_{\text{in}} = \overrightarrow{Z_0} \cdot \frac{\overrightarrow{Z_l} + \overrightarrow{Z_0} \cdot \tanh(\overrightarrow{\gamma} l)}{\overrightarrow{Z_0} + \overrightarrow{Z_l} \cdot \tanh(\overrightarrow{\gamma} l)} \tag{1}$$

where $\overrightarrow{Z_0}$ is the characteristic impedance of the line, l is the length of the transmission line, and $\overrightarrow{\gamma}$ the propagation constant that can easily be calculated using (2) and (3):

$$\overrightarrow{Z_0} = \sqrt{\frac{\overrightarrow{Z}}{\overrightarrow{Y}}} \tag{2}$$

$$\overrightarrow{\gamma} = \sqrt{\overrightarrow{Z} \cdot \overrightarrow{Y}} \tag{3}$$

where $\overrightarrow{Z}$ and $\overrightarrow{Y}$ correspond to the per unit length (p.u.l) series impedance and shunt admittance of the transmission line, respectively, which can be computed as described in [35].

Considering a branched topology, such as the one presented in Fig. 1, under normal operation conditions, hence, ignoring the presence of the fault, the respective line input impedance may be calculated with (4):

$$\overrightarrow{Z}_{\text{in}} = \overrightarrow{Z_0} \cdot \frac{\overrightarrow{Z}_{\text{eq}}^{(N-1)} + \overrightarrow{Z_0} \tanh(\overrightarrow{\gamma} l_N)}{\overrightarrow{Z_0} + \overrightarrow{Z}_{\text{eq}}^{(N-1)} \tanh(\overrightarrow{\gamma} l_N)} \tag{4}$$

where l_N is the length of the N_{th} branch, and $\overrightarrow{Z}_{\text{eq}}^{(N-1)}$ may be calculated using (5).

$$\overrightarrow{Z}_{\text{eq}}^{(N-1)} = \left(\overrightarrow{Z}_{\text{in}}^{(N-2)} // \overrightarrow{Z}_{\text{in}}^{(N-1)} \right) \tag{5}$$

$\overrightarrow{Z}_{\text{in}}^{(N)}$ may be calculated using (1), incorporating the suitable transmission line lengths and terminations. The necessary for the computation lengths of branches may be easily acquired in practice by a geographical information system (GIS) that contains the information for the studied topology.

When a HIF occurs at a distance l_{fault} from the beginning of the N_{th} branch, this branch may be divided into two different sections. The first section extends from the fault to the branch termination. The overall impedance of this line part is $\overrightarrow{Z}_{\text{end}}^{(N)}$, as shown in Fig. 1, and it may be calculated using (6). The second section consists of the length from the beginning of the branch to the fault location, and it is terminated to the parallel connection of the fault impedance, $\overrightarrow{Z}_{\text{fault}}$, and the impedance of the former branch section $\overrightarrow{Z}_{\text{end}}$. It should be noted, that for the purposes of this study it is valid to consider a constant fault impedance ($\overrightarrow{Z}_{\text{fault}}$), as the analyzed period corresponding to the frequency range under study is very small as compared to the changes in the HIF impedance value. This parallel connection will have an impedance $\overrightarrow{Z}_{\text{parallel}}$ as shown in (7). The total branch impedance $\overrightarrow{Z}_{\text{infault}}^{(N)}$ may then be calculated by (8). This new branch impedance may also be used with the procedure described by (4) and (5) for the computation of the new input impedance of the line under study.

$$\overrightarrow{Z}_{\text{end}}^{(N)} = \overrightarrow{Z_0} \cdot \frac{\overrightarrow{Z}_{\text{eq}}^{(N-1)} + \overrightarrow{Z_0} \cdot \tanh[\overrightarrow{\gamma}(l_N - l_{\text{fault}})]}{\overrightarrow{Z_0} + \overrightarrow{Z}_{\text{eq}}^{(N-1)} \cdot \tanh[\overrightarrow{\gamma}(l_N - l_{\text{fault}})]} \tag{6}$$

$$\overrightarrow{Z}_{\text{parallel}} = \overrightarrow{Z}_{\text{end}}^{(N)} /\!/ \overrightarrow{Z}_{\text{fault}} \tag{7}$$

$$\overrightarrow{Z}_{\text{infault}}^{(N)} = \overrightarrow{Z_0} \cdot \frac{\overrightarrow{Z}_{\text{parallel}} + \overrightarrow{Z_0} \cdot \tanh(\overrightarrow{\gamma} l_{\text{fault}})}{\overrightarrow{Z_0} + \overrightarrow{Z}_{\text{parallel}} \cdot \tanh(\overrightarrow{\gamma} l_{\text{fault}})} \tag{8}$$

The appearance of a high impedance fault to earth within the line will naturally affect the overall input impedance of the circuit. The difference between the normal input impedance $\overrightarrow{Z}_{\text{in}}$, i.e., when there is no fault across the line, and the one under fault conditions, i.e., $\overrightarrow{Z}_{\text{infault}}$, may be used to indicate the existence of a HIF. To this purpose, a function D_f, may be used, which is equal to the difference of the magnitudes of the two calculated impedances, as shown in (9), where f is frequency. Moreover, function D_p may further be used for the calculation of the percentage difference between the input impedance values of the two states.

$$D_f(f) = |\overrightarrow{Z}_{\text{in}}(f)| - |\overrightarrow{Z}_{\text{infault}}(f)| \tag{9}$$

$$D_p(f) = \frac{|\overrightarrow{Z}_{\text{infault}}(f)| - |\overrightarrow{Z}_{\text{in}}(f)|}{|\overrightarrow{Z}_{\text{in}}(f)|} \cdot 100\% \tag{10}$$

The functions D_f and D_p may also be used in the case of a broken conductor. In this case, however, the theoretical calculations have to be slightly adjusted. More specifically, broken conductors correspond to a cutoff phase wire that may be swaying in air, coming possibly in contact with objects in the vicinity of the power line. Naturally, the occurrence of a broken phase wire changes entirely the topology of the network and consequently the computed input impedance. Therefore, for this particular case the new formed circuit topology has to be considered taking into account that the phase wire is terminated to an open circuit or to a high impedance at the point that the conductor has been cut off, and that the rest of the network after that point is no longer part of the calculations. In more detail, in

confronting the broken conductor issue the procedure described by (6)–(8) would differ by the fact that $\overrightarrow{Z}_{\text{end}}^{(N)}$ is not needed because of the change in system topology, whereas $\overrightarrow{Z}_{\text{parallel}}$ is equal to $\overrightarrow{Z}_{\text{fault}}$, i.e., open circuit or high impedance.

The method proposed here for HIF detection consists of constantly measuring the input impedance of a given network topology, for a set of frequencies within the 3–95 kHz range. Subsequently, the values of D_f and D_p are constantly calculated in order to provide a criterion for HIF detection. As explained, the respective MV/LV power transformers will behave as open circuits, therefore the measured impedance values will depend on the MV network topology (constant under normal operational conditions), and the measurement equipment accuracy. This determines the threshold that may be used for HIF detection, as essentially any D_p value clearly exceeding the standard accuracy of the measuring device will indicate a fault occurrence.

Having determined that, there remains a question regarding the limitations of the proposed method. These limitations may correspond to false positive alerts (i.e., indications of a fault that doesn't exist), or false negative alerts respectively (i.e., failure to indicate a fault occurrence). A false positive alert could occur during a self-clearing fault (e.g., a thunderbolt hitting the line), or during a change in the network topology (e.g., a network reconfiguration). However, the former could be easily confronted, as the continuous monitoring of the network input impedance would indicate the clearing of the impermanent fault, while the latter would be known to the distribution network operator. On the other hand, a false negative alert is possible in the case of a fault with such high impedance, that the effect on the network is negligible (a natural limit for any HIF detection technique). Thus it may be concluded that the proposed system will work on all practical cases. Unfortunately, the nature of the problem does not allow for a clear mathematical determination of the aforementioned limitations, due to the inherent lack of information concerning the complex parameters involved (such as the probability of the fault occurring at a specific point of the line, with a specific fault impedance).

For the actual implementation of the proposed method, the important thing is not the exact theoretical calculation of the input impedance of each phase, but rather the fact that this input impedance will have an almost constant value that will substantially change only in the presence of the fault (regarding the MV network topology, as explained in Section II-A). The proposed method relies thus in the constant measurement of this input impedance, and the decision making procedure upon the occurrence of any abnormality in its value. The application of the method requires the superposition of a specific voltage signal onto the monitored network, and the measurement of both the superimposed voltage and the corresponding input current of the topology for specific frequencies. The necessary equipment for the application of the method constitutes of voltage and current measuring devices of high sampling rate, sufficient in order to cope with the high frequencies utilized. This equipment is expected to provide the input impedance value at the studied frequency range. Normally, respective coupling devices would be also needed, but in this case the couplers of the already existing PLC devices may be used to that purpose.

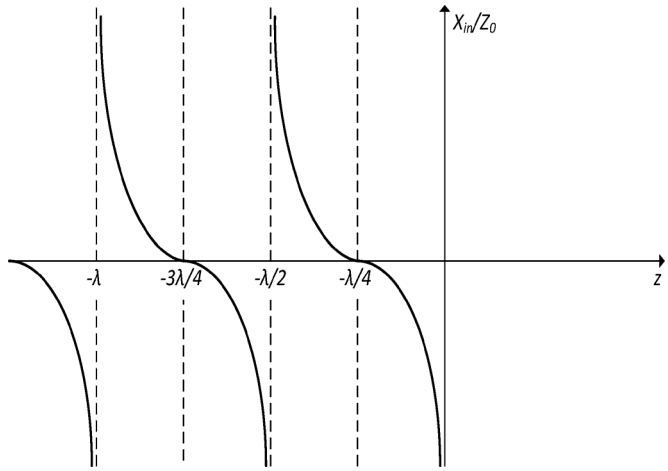

Fig. 2. Ratio of line's input reactance to the respective characteristic impedance, versus the line length.

C. Frequency Selection

Functions D_f and D_p may be used for the detection of a HIF. Their values however are frequency dependent. Therefore, a methodology has to be developed in order to determine the optimum frequencies to be used, i.e., the frequencies at which these functions will take their maximum values. Considering an open ended lossless transmission line (corresponding to a MV power line terminated at a distribution transformer), standing waves are created along its length z. The voltage and current expressions on the line are given by (11) and (12) [36]:

$$\overrightarrow{V}(z) = V_0^+ \cdot (e^{-j\beta z} + e^{j\beta z}) \tag{11}$$

$$\overrightarrow{I}(z) = \frac{V_0^+}{Z_0} \cdot (e^{-j\beta z} + e^{j\beta z}) \tag{12}$$

where V_0^+ is the amplitude of the incident field generated from a source and traveling towards the open end of the line. Moreover, β corresponds to the imaginary part of the propagation constant. The combination of these expressions results to an alternating value of the input impedance along the transmission line's length, which may be calculated with (27).

$$\overrightarrow{Z}_{\text{in}}(z) = -jZ_0\cot(\beta z) \tag{13}$$

This expression indicates a constant change to the input impedance at different points of the transmission line, as also shown in Fig. 2, in which the ratio $(X_{\text{in}})/(Z_0)$ is plotted versus the line length. As it is illustrated in the figure, the standing wave pattern created results in a rise in the input impedance value at specific points related to the wavelength value for the frequency considered. The exact position of these peaks varies for different frequencies due to the respective wavelength alteration.

The input impedance values which change with the frequency may be exploited for the HIF detection procedure. More specifically, they may be used in order to produce a desirable for the

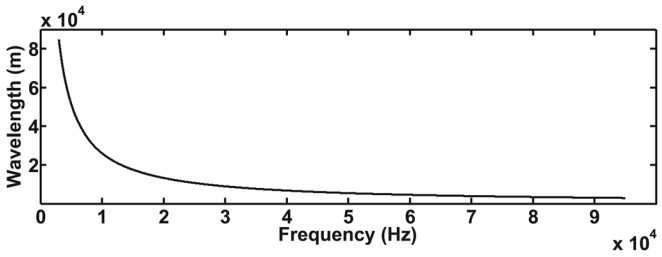

Fig. 3. Wavelength for every frequency of the chosen range.

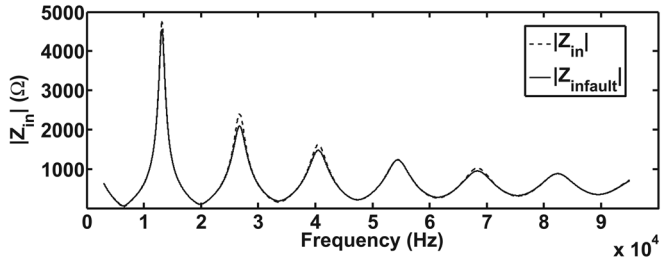

Fig. 4. Magnitude of input impedance under normal and fault conditions, for a case of a HIF of 15 kΩ, occurring at 6 km of a 10 km line.

HIF detection value of $\overrightarrow{Z}_{\rm end}$, as it is calculated in (20). This impedance is connected in parallel with the fault impedance, resulting in the $\overrightarrow{Z}_{\rm parallel}$ value of (7). As it is obvious, the closer the value of $\overrightarrow{Z}_{\rm end}$ to the fault impedance value, the greater the difference in the network total input impedance, as compared to its normal value.

The problem of HIF detection reduces thus to the determination of a suitable frequency band to be used for the monitoring of the network input impedance value. Utilities may use the Cenelec A frequency band, i.e., 9–95 kHz, as well as the range 3–9 kHz, for operational purposes. The wavelengths corresponding to these frequency ranges are plotted versus frequency in Fig. 3. As it may be observed in this figure, these wavelengths vary from tens of kilometers to kilometers, and are suitable hence for typical rural medium voltage feeder lengths ranging within several tens of km [37]. It may be deducted thus that the monitoring of a combination of certain frequencies within the aforementioned ranges may provide an effective way of HIF detection.

D. Effect of Earth's Electromagnetic Properties on the Proposed Method's Efficacy

The proposed method makes use of the ground plane as a return path for the circuit formed for HIF detection, utilizing frequencies much higher than the main operational frequency of the network. Along the large distances of distribution feeders, the electromagnetic properties of the earth, i.e., earth's conductivity σ_g and permittivity ε_g, may vary. Prior knowledge of these properties, and of the possible changes in their values at different areas, is practically impossible, therefore the effect of these variations to the method's efficacy has to be investigated.

These electromagnetic properties influence the ground impedance and admittance values, and thus the total per unit length transmission line impedance and admittance [38], [39]. However, these quantities are not that important for the chosen frequency range, as they exhibit values that are much smaller than the external impedance and admittance respectively. Therefore, the variations in ground conductivity and permittivity are expected to have an insubstantial effect on the method results.

III. Calculations

A variety of parameters are involved in the process of the HIF detection methodology proposed here. These parameters include the network topology, the HIF impedance value and location, and the electromagnetic properties of the earth. Therefore, simulations with typical values of all these factors have been conducted here. The aim of these simulations is to evaluate the efficiency of the method, ensuring that in any HIF case the resulting network input impedance will significantly variate from its respective normal value in the selected frequency range, making thus the HIF detection possible.

The simulations are grouped into two basic test cases. In the first one, results concerning overhead MV transmission lines with no branches are presented, so as to test the validity of the model. Subsequently, in the second test case, the method is applied to a transmission line that is part of the Greek electrical network. If it is not stated otherwise, the earth's resistivity and relative permittivity are considered equal to 100 Ωm and 10 respectively. All simulations regarding frequency and time domain results have been conducted using source code written in Matlab R2011a 64 bit edition and SimPowerSystems toolbox of the corresponding Matlab/Simulink platform, respectively.

A. Single Branch Topologies

At first, an indicative case will be presented, in order to clarify the theoretical analysis of Section II. This case corresponds to a HIF value of 15 kΩ, occurring at 6 km of a 10 km line. In Fig. 4, the absolute values of the line input impedance under normal operation, as well as its respective value under HIF conditions, are plotted versus frequency. The resulting curves are constantly changing as the electromagnetic properties of the transmission line are not constant with frequency, presenting a parabola type pattern, but with different maximum values. It can be noticed that divergences between the two impedances occur at the curve notches. Moreover, in Fig. 5 the functions D_f and D_p corresponding to the same case are plotted. Both functions follow the same pattern. The most important observation is that large deviations in absolute values (function D_f) may correspond to small percentage deviations (function D_p), while small deviations in absolute values may correspond to large percentage ones. Significant divergences occur at specific frequencies, the utilization of which could lead to effective HIF monitoring. Specifically, D_p exhibits a maximum value of about 60% at a frequency close to 9 kHz.

A significant issue that has to be confronted is the effect of the fault's location to the efficacy of the method. Thus, the second case presented corresponds to all possible fault locations at a 25 km long transmission line, for a HIF value of 5 kΩ. Results regarding this case are presented in Fig. 6, in a three dimensional graph containing the frequency variation in x axis, the fault lo-

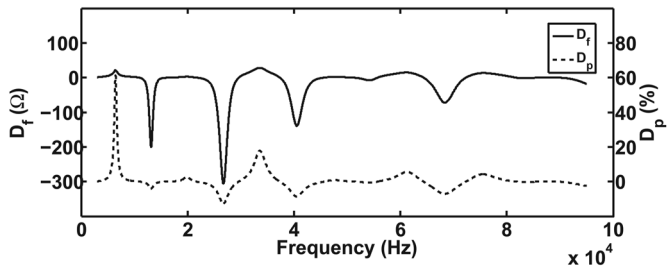

Fig. 5. Functions D_f and D_p versus frequency, for a case of a HIF of 10 kΩ, occurring at 6 km of a 10 km line.

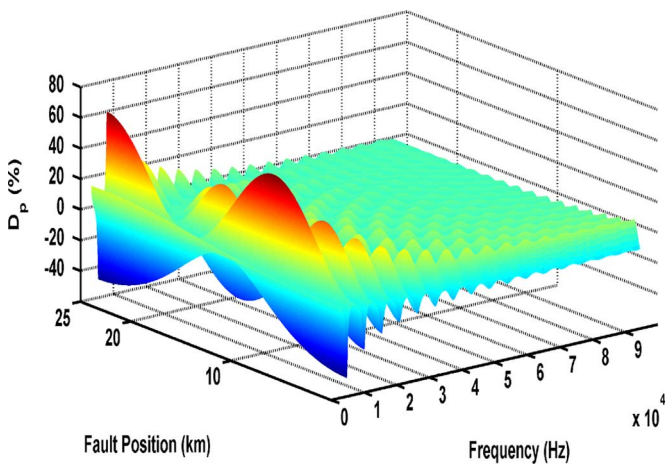

Fig. 6. Effect of various fault locations of a 5 kΩ fault to the value of D_p function, considering a line of 25 km.

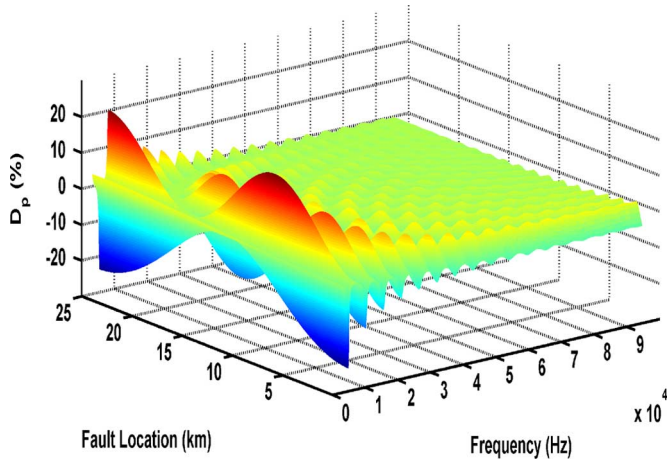

Fig. 7. Effect of various fault positions of a 15 kΩ fault to the value of D_p function, considering a line of 25 km.

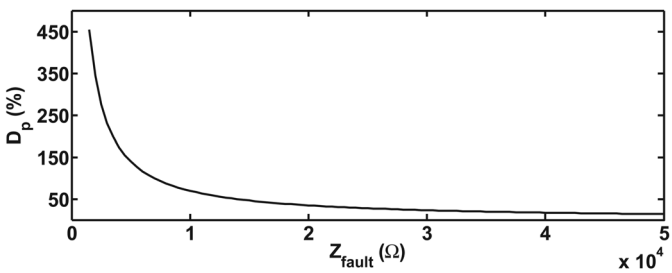

Fig. 8. Effect of various fault impedances to the value of D_p function, for the case of a HIF occurring at 10 km of a 15 km line.

cation in y axis, and values of function D_p in z axis. The graph presents this specific form because of the standing waves in the line, and it can be noticed that certain frequencies perform adequately for some fault locations, and fail for others. However, this drawback may be overcome by choosing more than one frequency for the monitoring of the entire length of the line. As it is shown in the figure a combination of two or three frequencies may perform well exhibiting deviations more than 30% in the pre-fault and after-fault values of the line input impedances.

In Fig. 7, results are shown concerning the same case, but for a HIF value of 15 kΩ, in order to investigate the effect of HIF value to the method's effectiveness. As it may be observed in the figure, the same pattern appears as in Fig. 6, with the same frequencies exhibiting optimum performance. In this case however, smaller deviations are detected, confirming that, as the HIF value increases, the method's capability of detection is reduced. However, the computed divergences are large enough for the effective application of the method.

The next test case aims to further investigate the influence of the HIF value to the method results. To this purpose, a line is investigated with a total length of 15 km. A HIF is considered to occur at 10 km from the line starting point, with an impedance value ranging from 1.5 kΩ to 50 kΩ. Results for this case are presented in Fig. 8, where function D_p is plotted versus HIF impedance values. Substantial deviations may be observed in this figure for smaller impedance values, whereas these values decline with the increase of the HIF value, reaching a minimum of about 10%. It is important to remark that all the maximum percentage deviations were exhibited in this case for a single frequency, strongly indicating thus that for every fault location there is a single frequency which performs best, almost independently of the HIF value.

In Figs. 9 and 10, results are presented for the case of faults corresponding to broken line conductors. More specifically, in Fig. 9, the function D_p is plotted versus frequency and broken conductor location at the second half of a 30 km long line. Similarly, in Fig. 10 the same results are illustrated for the first half of the same power line. As it may be observed, the D_p values in this case are very large, permitting thus the usage of the proposed method for the detection of broken conductors. Once again, the monitoring of more than one frequency could provide full coverage for the total line length. It is very interesting to observe that these large deviations are recorded at the same frequencies that could be also used for simple HIF detection. These frequencies could thus serve for both HIF and broken conductor detection for each line topology. As expected, maximum values are recorded when the location of the broken conductor is close to the line starting point. The actual obtained values were even larger, therefore they were downscaled, in order for the better depiction of the respective results at the rest of the frequencies.

Moreover, Figs. 11 and 12 depict the effect of variations of the earth's electromagnetic properties to the method's efficacy. The results come from a 20 kΩ fault at the middle of a 20 km line. As it was described in Section II, the variation in earth resistivity affects the line electromagnetic characteristics through the change in the ground impedance and admittance. As it is shown, this alteration in value does not significantly influence the efficacy of

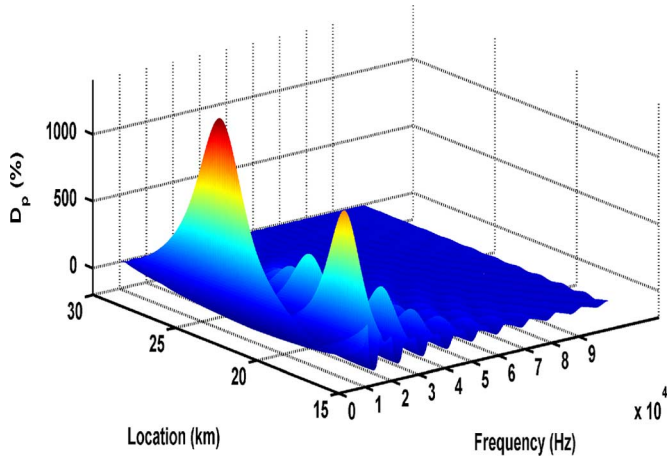

Fig. 9. Effect of various broken conductor locations to the value of D_p function, for the second half of a 30 km line.

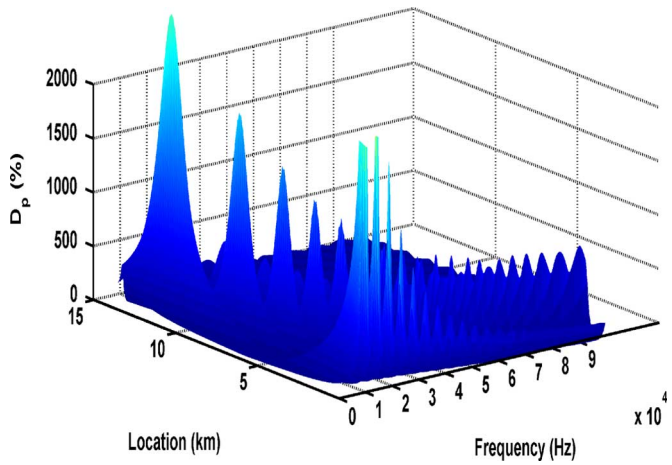

Fig. 10. Effect of various broken conductor positions to the value of D_p function, for the first half of a 30 km line.

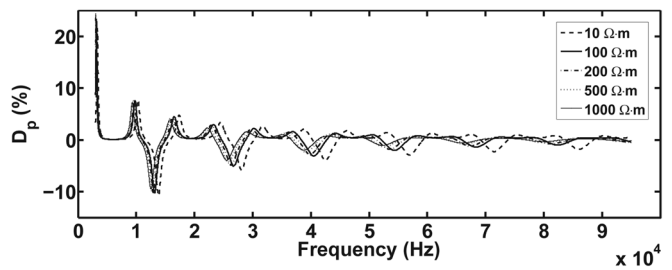

Fig. 11. Effect of the variation in earth resistivity on the value of D_p, for a 20 kΩ fault at the middle of a 20 km line.

the method. The illustrated curves practically follow the same pattern and exhibit the same values, with a slight phase difference. The curve that corresponds to the highest regarded value of earth conductivity exhibits a slightly differentiated behavior, while the three curves corresponding to the most common resistivity values are identical. Nevertheless, the highest recorded values appear at adjacent frequencies for all cases. Thus, the usage of the same frequencies can cover a variety of different resistivity cases. Alternatively, monitoring small frequency subranges could perform effectively for HIF detection.

In Fig. 12 the effect of earth's relative permittivity to the application of the method is finally shown. It can be easily concluded that different values of permittivity leave the results unaffected, as the computed D_p values, as well as the optimum frequencies, coincide.

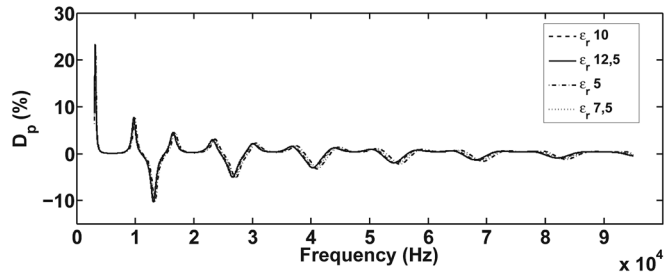

Fig. 12. Effect of the variation in earth permittivity on the value of D_p, for a 20 kΩ fault at the middle of a 20 km line.

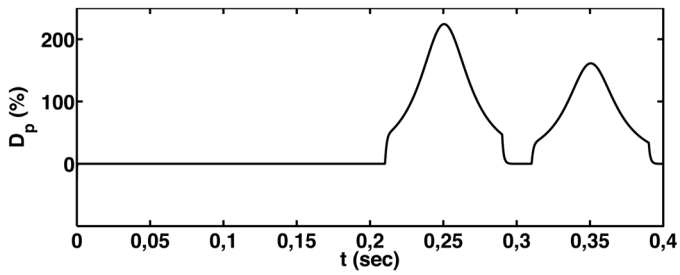

Fig. 13. Effect of arcing fault occurrence at the middle of a 20 km line on the value of D_p.

Furthermore, it is very interesting to investigate the case of occurring arcing fault as it is explained in [40]. The arcing fault is considered to be located at the middle of a 20 km line and the simulation has been conducted using the Matlab/Simulink software. In Fig. 13 the deviation of function D_p, calculated for the best performing frequency for the specific fault location of the transmission line as it is depicted from Fig. 12 (i.e., 3165 Hz), is plotted versus time. The arcing fault initiates at the time of 0.2 sec and after that a period of the fundamental frequency (50 Hz) is shown. It is observed that the deviation, illustrated by D_p, is significant, making detection of such kind of faults possible, and exhibits a maximum value of 224% for the positive half period and 161.3% for the negative half period of the fundamental frequency, respectively.

B. Multibranch Topologies

An actual topology with a number of branches was also selected for the evaluation of the proposed method, in order to investigate its efficiency under realistic conditions. More specifically, the topology selected to be simulated is part of the Greek rural MV distribution network, located outside of the city of Thessaloniki. The network under study is illustrated in Fig. 14, and the lengths of all branches are listed in Table I. Its nominal voltage is 20 kV and the phase wires are ACSR conductors of 70/12 mm^2 nominal cross section at a height of 10 m above the ground plane.

In Fig. 15, D_p values are plotted for the case of a HIF value of 20 kΩ occurring at various points of the selected feeder. The fault was selected to be at 3, 6, 9, and 12 km from the line starting point. It is shown that for every tested case the computed D_p values are again substantial, and the application of the method can be once more simplified by choosing to monitor specific

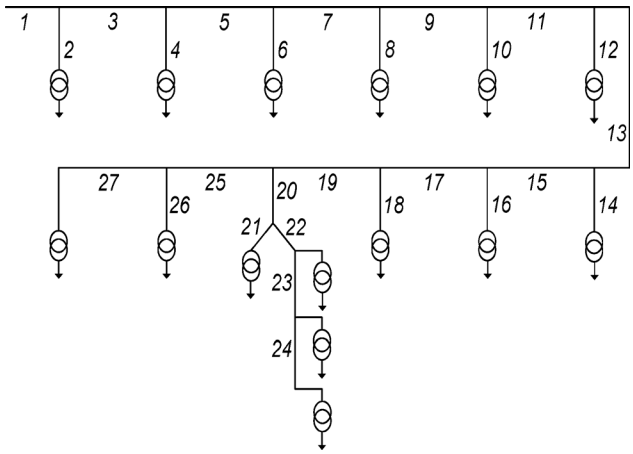

Fig. 14. Real topology configuration.

TABLE I
BRANCHES LENGTHS

Branch number	Length (m)	Branch number	Length (m)
1	2100	15	1100
2	20	16	20
3	390	17	1300
4	130	18	20
5	1200	19	1100
6	160	20	700
7	2100	21	30
8	10	22	1200
9	300	23	780
10	720	24	220
11	1100	25	580
12	120	26	70
13	1500	27	1500
14	400	-	-

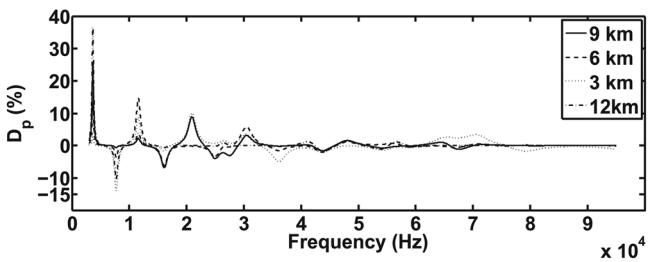

Fig. 15. Effect of various 20 kΩ fault locations to the value of D_p function.

frequencies rather than the whole frequency range, in order to cover the total length of the line. The same conclusion can also be derived by studying Fig. 16. This graph contains the computed D_p values for every possible location of a 10 kΩ HIF along the feeder length. The existence of the fault affects again considerably the input impedance of the network, and once more it is sufficient to monitor a small number of frequencies for HIF detection at every point of the feeder. These few frequencies may also be used for broken conductor detection, as it is shown in Fig. 17. In more detail, in this figure the D_p values for different locations of a broken conductor along the feeder under study are plotted. The magnitude of the D_p values observed in

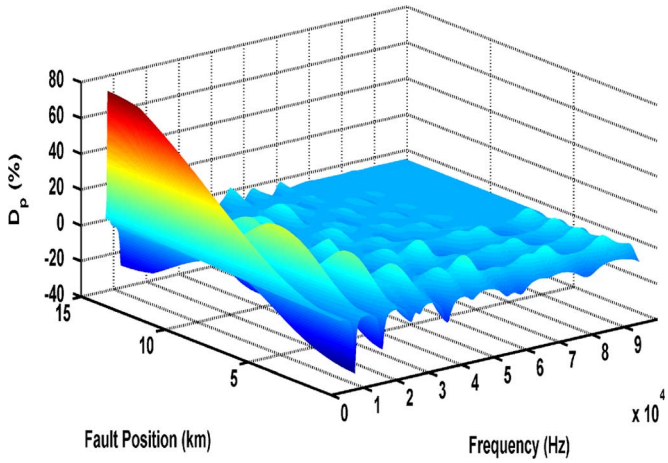

Fig. 16. Effect of various 10 kΩ fault locations to the value of D_p function.

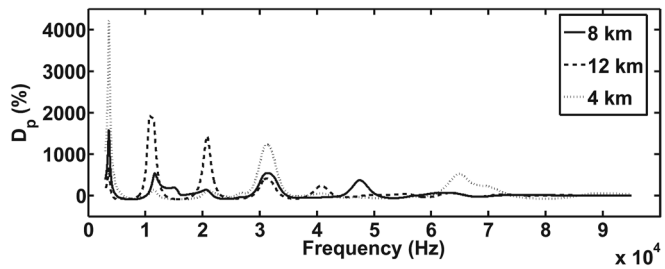

Fig. 17. Effect of various broken conductor locations to the value of D_p function.

this case is very large, enabling thus the easy fault detection with the proposed method. As it was also concluded from the simulation of the proposed method in single branch topologies, the closer the broken conductor is to the starting point of the line, the easier the detection.

IV. CONCLUSION

A novel method for the detection of high impedance fault occurrence in overhead rural distribution networks is presented. This method could be easily comprised as a first step in a procedure, which utilizes power line communication technology in order to offer both HIF detection and location. The HIF detection concept is presented here, while the respective HIF location concept is analyzed in Part II of this work.

The HIF detection method utilizes signal superposition on the power lines, in a frequency band that may be used by electric power utilities for data transmission. Significant deviations between input impedances under normal and fault conditions are detected for the selected frequency range. These divergences may be used by a system for HIF detection, which will essentially scan all the selected frequencies on a given power line. It is concluded that the method performs satisfactorily for a wide variety of cases. It is also shown that the effect of the earth, which is used as a return path for the method's circuit formulation, is negligible. Furthermore, the application of the method can be simplified by using few single frequencies, each of which performs best for a specific part of a power line. This frequency combination enhances the possible application of the method.

Moreover, the case of broken conductors is also examined and a satisfactory performance is observed.

ACKNOWLEDGMENT

The authors would like to thank Mrs. S. Fahouridis and A. Zafirakis of the Public Power Corporation (PPC) of Greece for providing the needed data that enabled this study to be conducted successfully.

REFERENCES

[1] J. Tengdin, R. Westfall, and K. Stephan, "High impedance fault detection technology," Rep. PSRC Working Group D, 1996, vol. 15.
[2] J. de Sa and M. Louro, "On human life risk-assessment and sensitive ground fault protection in mv distribution networks," *IEEE Trans. Power Del.*, vol. 25, no. 4, pp. 2319–2327, 2010.
[3] M. Aucoin, "Status of high impedance fault detection," *IEEE Trans. Power App. Syst.*, vol. PAS-104, no. 3, pp. 637–644, 1985.
[4] L. Li and M. Redfern, "A review of techniques to detect downed conductors in overhead distribution systems," in *Proc. 7th Int. Conf. Develop. Power Syst. Protection 2001 (IEE)*.
[5] B. M. Aucoin and B. D. Russell, "Distribution high impedance fault detection utilizing high frequency current components," *IEEE Power Eng. Rev.*, vol. PER-2, no. 6, pp. 46–47, 1982.
[6] M. Aucoin and B. D. Russell, "Detection of distribution high impedance faults using burst noise signals near 60 hz," *IEEE Trans. Power Del.*, vol. 2, no. 2, pp. 342–348, 1987.
[7] R. Lee and R. Osborn, "A microcomputer based data acquisition system for high impedance fault analysis," *IEEE Trans. Power App. Syst.*, vol. PAS-104, no. 10, pp. 2748–2753, 1985.
[8] R. Lee and M. Bishop, "A comparison of measured high impedance fault data to digital computer modeling results," *IEEE Trans. Power App. Syst.*, vol. PAS-104, no. 10, pp. 2754–2758, 1985.
[9] S. J. Balser, K. A. Clements, and D. J. Lawrence, "A microprocessor-based technique for detection of high impedance faults," *IEEE Trans. Power Del.*, vol. 1, no. 3, pp. 252–258, 1986.
[10] N. Elkalashy, A. Elhaffar, T. Kawady, N. Tarhuni, and M. Lehtonen, "Bayesian selectivity technique for earth fault protection in medium-voltage networks," *IEEE Trans. Power Del.*, vol. 25, no. 4, pp. 2234–2245, 2010.
[11] N. Elkalashy, M. Lehtonen, H. Darwish, A.-M. Taalab, and M. Izzularab, "Dwt-based detection and transient power direction-based location of high-impedance faults due to leaning trees in unearthed mv networks," *IEEE Trans. Power Del.*, vol. 23, no. 1, pp. 94–101, 2008.
[12] C.-H. Kim, H. Kim, Y.-H. Ko, S.-H. Byun, R. Aggarwal, and A. Johns, "A novel fault-detection technique of high-impedance arcing faults in transmission lines using the wavelet transform," *IEEE Trans. Power Del.*, vol. 17, no. 4, pp. 921–929, Oct. 2002.
[13] D. C. T. Wai and X. Yibin, "A novel technique for high impedance fault identification," *IEEE Trans. Power Del.*, vol. 13, no. 3, pp. 738–744, Jul. 1998.
[14] T. Lai, L. Snider, E. Lo, and D. Sutanto, "High-impedance fault detection using discrete wavelet transform and frequency range and rms conversion," *IEEE Trans. Power Del.*, vol. 20, no. 1, pp. 397–407, Jan. 2005.
[15] M. Michalik, M. Lukowicz, W. Rebizant, S.-J. Lee, and S.-H. Kang, "Verification of the wavelet-based hif detecting algorithm performance in solidly grounded mv networks," *IEEE Trans. Power Del.*, vol. 22, no. 4, pp. 2057–2064, 2007.
[16] M. Michalik, M. Lukowicz, W. Rebizant, S.-J. Lee, and S.-H. Kang, "New ann-based algorithms for detecting hifs in multigrounded mv networks," *IEEE Trans. Power Del.*, vol. 23, no. 1, pp. 58–66, 2008.
[17] A. Sultan, G. Swift, and D. Fedirchuk, "Detection of high impedance arcing faults using a multi-layer perceptron," *IEEE Trans. Power Del.*, vol. 7, no. 4, pp. 1871–1877, Oct. 1992.
[18] J.-H. Ko, J.-C. Shim, C.-W. Ryu, C.-G. Park, and W.-Y. Yim, "Detection of high impedance faults using neural nets and chaotic degree," in *Proc. Int. Conf. Energy Manage. Power Del. (EMPD)*, Mar. 1998, vol. 2, pp. 399–404, vol. 2.
[19] P. Jota and F. Jota, "Fuzzy detection of high impedance faults in radial distribution feeders," *Elect. Power Syst. Res.*, vol. 49, no. 3, pp. 169–174, 1999.
[20] A. Bose, "Smart transmission grid applications and their supporting infrastructure," *IEEE Trans. Smart Grid*, vol. 1, no. 1, pp. 11–19, 2010.
[21] P. Zhang, F. Li, and N. Bhatt, "Next-generation monitoring, analysis, and control for the future smart control center," *IEEE Trans. Smart Grid*, vol. 1, no. 2, pp. 186–192, 2010.
[22] F. Li, W. Qiao, H. Sun, H. Wan, J. Wang, Y. Xia, Z. Xu, and P. Zhang, "Smart transmission grid: Vision and framework," *IEEE Trans. Smart Grid*, vol. 1, no. 2, pp. 168–177, 2010.
[23] G. Heydt, "The next generation of power distribution systems," *IEEE Trans. Smart Grid*, vol. 1, no. 3, pp. 225–235, 2010.
[24] W. Gao and J. Ning, "Wavelet-based disturbance analysis for power system wide-area monitoring," *IEEE Trans. Smart Grid*, vol. 2, no. 1, pp. 121–130, Mar. 2011.
[25] M. Kezunovic, "Smart fault location for smart grids," *IEEE Trans. Smart Grid*, vol. 2, no. 1, pp. 11–22, Mar. 2011.
[26] S. Galli, A. Scaglione, and Z. Wang, "For the grid and through the grid: The role of power line communications in the smart grid," *Proc. IEEE*, vol. 99, no. 6, pp. 998–1027, Jun. 2011.
[27] P. Amirshahi and M. Kavehrad, "High-frequency characteristics of overhead multiconductor power lines for broadband communications," *IEEE J. Sel. Areas Commun.*, vol. 24, no. 7, pp. 1292–1303, Jul. 2006.
[28] J. Anatory, N. Theethayi, R. Thottappillil, M. Kissaka, and N. Mvungi, "Broadband power-line communications: The channel capacity analysis," *IEEE Trans. Power Del.*, vol. 23, no. 1, pp. 164–170, Jan. 2008.
[29] A. Lazaropoulos and P. Cottis, "Capacity of overhead medium voltage power line communication channels," *IEEE Trans. Power Del.*, vol. 25, no. 2, pp. 723–733, Apr. 2010.
[30] M. Zimmermann and K. Dostert, "A multipath model for the powerline channel," *IEEE Trans. Commun.*, vol. 50, no. 4, pp. 553–559, Apr. 2002.
[31] I. Zamora, A. Mazon, K. Sagastabeitia, and J. Zamora, "New method for detecting low current faults in electrical distribution systems," *IEEE Trans. Power Del.*, vol. 22, no. 4, pp. 2072–2079, Oct. 2007.
[32] J. Zamora, I. Zamora, A. Mazon, and K. Sagastabeitia, "Optimal frequency value to detect low current faults superposing voltage tones," *IEEE Trans. Power Del.*, vol. 23, no. 4, pp. 1773–1779, Oct. 2008.
[33] A. Milioudis, G. Andreou, and D. Labridis, "High impedance fault detection using power line communication techniques," in *Proc. 45th Int. Univ. Power Eng. Conf. (UPEC)*, 31 2010–Sep. 3 2010, pp. 1–6.
[34] R. Matick, *Transmission Lines for Digital and Communication Networks*. New York: McGraw-Hill, 1969.
[35] M. D'Amore and M. Sarto, "Simulation models of a dissipative transmission line above a lossy ground for a wide-frequency range. i. single conductor configuration," *IEEE Trans. Electromagn. Compat.*, vol. 38, no. 2, pp. 127–138, May 1996.
[36] D. Pozar, *Microwave Engineering*, 2nd ed. New York: Wiley, 1998.
[37] D. Cortinas *et al.*, "Fault management in electrical distribution systems," CIRED Working Group WG03 Fault Management, Final Rep., 1998.
[38] T. Papadopoulos, G. Papagiannis, and D. Labridis, "Wave propagation characteristics of overhead conductors above imperfect stratified earth for a wide frequency range," *IEEE Trans. Magn.*, vol. 45, no. 3, pp. 1064–1067, 2009.
[39] T. Papadopoulos and G. Papagiannis, "Influence of earth permittivity on overhead transmission line earth-return impedances," in *Proc. IEEE Lausanne Power Tech. Conf.*, Jul. 2007, pp. 790–795.
[40] M. Michalik, W. Rebizant, M. Lukowicz, S.-J. Lee, and S.-H. Kang, "High-impedance fault detection in distribution networks with use of wavelet-based algorithm," *IEEE Trans. Power Del.*, vol. 21, no. 4, pp. 1793–1802, Oct. 2006.

Apostolos N. Milioudis was born in Xanthi, Greece, on February 27, 1985. He received the Dipl.-Eng. degree from the Department of Electrical and Computer Engineering at the Aristotle University of Thessaloniki, Greece, in 2007. He is currently working toward the Ph.D. degree at the same university.

His special interests are power system analysis with special emphasis on the simulation of transmission and distribution systems, high impedance fault detection techniques, artificial intelligence applications in power systems, and power line communications.

Georgios T. Andreou (S'98–A'02–M'08) was born in Thessaloniki, Greece, on August 16, 1976. He received the Dipl.-Eng. and Ph.D. degrees from the Department of Electrical and Computer Engineering at the Aristotle University of Thessaloniki in 2000 and 2006, respectively.

Currently he is a Lecturer at the same Department. His special interests are power system analysis with special emphasis on the simulation of transmission and distribution systems, electromagnetic and thermal field analysis, and power line communications.

Dimitrios D. Labridis (S'88–M'90–SM'00) was born in Thessaloniki, Greece, on July 26, 1958. He received the Dipl.-Eng. and the Ph.D. degrees from the Department of Electrical and Computer Engineering, Aristotle University of Thessaloniki, Greece, in 1981 and 1989, respectively.

Since 1990 he has been with the Electrical Engineering Department, Aristotle University of Thessaloniki, where he is currently a Professor. His research interests are power system analysis with special emphasis on the simulation of transmission and distribution systems.